

# Hedgehog Spin-vortex Crystal Antiferromagnetic Quantum Criticality in $\text{CaK}(\text{Fe}_{1-x}\text{Ni}_x)_4\text{As}_4$ Revealed by NMR

Q.-P. Ding,<sup>1,2</sup> W. R. Meier,<sup>1,2</sup> J. Cui\*,<sup>1,3</sup> M. Xu,<sup>1,2</sup> A. E. Böhmer†,<sup>1,2</sup> S. L. Bud'ko,<sup>1,2</sup> P. C. Canfield,<sup>1,2</sup> and Y. Furukawa<sup>1,2</sup>

<sup>1</sup>Ames Laboratory, U.S. DOE, Ames, Iowa 50011, USA

<sup>2</sup>Department of Physics and Astronomy, Iowa State University, Ames, Iowa 50011, USA

<sup>3</sup>Department of Chemistry, Iowa State University, Ames, Iowa 50011, USA

(Dated: June 6, 2021)

Two ordering states, antiferromagnetism and nematicity, have been observed in most iron-based superconductors (SCs). In contrast to those SCs, the newly discovered SC  $\text{CaK}(\text{Fe}_{1-x}\text{Ni}_x)_4\text{As}_4$  exhibits an antiferromagnetic (AFM) state, called hedgehog spin-vortex crystal structure, without nematic order, providing the opportunity for the investigation into the relationship between spin fluctuations and SC without any effects of nematic fluctuations. Our <sup>75</sup>As nuclear magnetic resonance studies on  $\text{CaK}(\text{Fe}_{1-x}\text{Ni}_x)_4\text{As}_4$  ( $0 \leq x \leq 0.049$ ) revealed that  $\text{CaKFe}_4\text{As}_4$  is located close to a hidden hedgehog SVC AFM quantum-critical point (QCP). The magnetic QCP without nematicity in  $\text{CaK}(\text{Fe}_{1-x}\text{Ni}_x)_4\text{As}_4$  highlights the close connection of spin fluctuations and superconductivity in iron-based SCs. The advantage of stoichiometric composition also makes  $\text{CaKFe}_4\text{As}_4$  an ideal platform for further detailed investigation of the relationship between magnetic QCP and superconductivity in iron-based SCs without disorder effects.

PACS numbers:

The relationship between antiferromagnetism (AFM), nematicity, and superconductivity in iron-based superconductors (SCs) has received wide interest [1–4]. The most controversial and important topic in iron-based SCs is the pairing mechanism, for which both spin and nematic fluctuations have been proposed, but no conclusion has been reached yet. SC in most iron-pnictides appears in proximity to an AFM ordered state, which is closely accompanied by a nematic order. The SC critical temperature,  $T_c$ , shows a dome-shaped dependence on carrier doping or pressure application. Heavy fermions and high- $T_c$  cuprates also exhibit similar phase diagrams [5, 6]. In these compounds, normal-state properties often show a striking deviation from Landau's Fermi liquid behavior near the optimal  $T_c$  composition [5–9]. The non-Fermi liquid behavior, such as temperature ( $T$ )-linear resistivity has been discussed in terms of a quantum critical point (QCP) [7, 10, 11]. The existence of magnetic QCP has been reported in several iron-pnictide SCs, such as  $\text{BaFe}_2\text{As}_2$ -type (122) systems, for example,  $\text{BaFe}_2(\text{As}_{1-x}\text{P}_x)_2$  [9, 12],  $\text{Ba}(\text{Fe}_{1-x}\text{M}_x)_2\text{As}_2$  ( $M = \text{Co}, \text{Ni}$ ) [13–15]. However, recent NMR,  $\mu\text{SR}$  and neutron scattering measurements indicate the presence of inhomogeneous AFM domains near optimal SC, suggesting an avoided QCP in electron-doped  $\text{Ba}(\text{Fe}_{1-x}\text{M}_x)_2\text{As}_2$  [16–20]. The inhomogeneity presumably originates from the disorder due to Ni/Co substitutions. Even though sub-

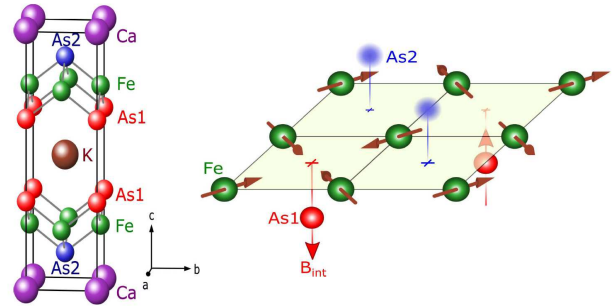


FIG. 1: The crystal structure of  $\text{CaKFe}_4\text{As}_4$  (left) and the sketch of hedgehog SVC spin structure on an Fe-As layer (right). The wine arrows represent the magnetic moments at the Fe sites and the red arrows represent the magnetic induction  $B_{\text{int}}$  at the As1 sites.

stitutional disorder is not introduced on the Fe plane in  $\text{BaFe}_2(\text{As}_{1-x}\text{P}_x)_2$ , a recent study combined with NMR, x-ray, and neutron diffraction measurements also suggests an avoided QCP [21]. Thus whether or not a magnetic QCP exists in 122 compounds is still under debate. On the other hand, nematic fluctuations associated with nematic QCP have been increasingly suggested to enhance or even lead to SC in iron-based SCs, especially 122 systems [22–24].

Different from the 122 family, the newly discovered stoichiometric iron-based SC  $\text{CaKFe}_4\text{As}_4$  with  $T_c \sim 35$  K adopts a structure where the Fe-As layers are separated by alternate Ca and K planes [25, 26]. The segregation of Ca and K is driven by their dissimilar sizes and reduces the space group from  $I4/mmm$  in 122 compounds to  $P4/mmm$  in  $\text{CaKFe}_4\text{As}_4$ . Consequently, as shown in the left panel of Fig. 1, there are two inequivalent As

\*Present address: Department of Chemistry, University of Delaware, Newark, Delaware 9716, USA

†Present address: Karlsruhe Institute of Technology, Institut für Festkörperphysik, 76021 Karlsruhe, Germany

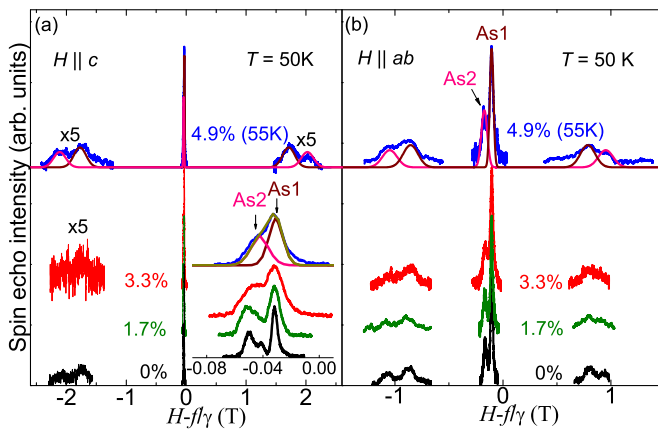


FIG. 2: Field-swept  $^{75}\text{As}$ -NMR spectra of  $\text{CaK}(\text{Fe}_{1-x}\text{Ni}_x)_4\text{As}_4$  at 50 K (55 K for 4.9% sample), for  $H \parallel c$  axis (a) and  $H \parallel ab$  plane (b). The inset in (a) enlarges the central transition. Pink and wine curves represent simulated spectra for As1 and As2, respectively. The dark yellow in the inset of (a) represents the sum of the simulated spectra.

sites: As1 and As2 sites close to the K and Ca layers, respectively. Other than SC, there is no indication of any other phase transition from 1.5 K to 300 K [26, 27]. The multiband nature of the compound and  $s\pm$  nodeless two-gap SC state has been revealed by various techniques [28–32]. Quite recently, a new magnetic state called hedgehog spin-vortex crystal (SVC) with tetragonal symmetry, as shown in the right panel of Fig. 1, has been discovered in the electron doped SC  $\text{CaK}(\text{Fe}_{1-x}\text{M}_x)_4\text{As}_4$  ( $M = \text{Co}$  or  $\text{Ni}$ ) [33]. The magnetic phase transition has been shown to be second order [33]. The subsequent NMR and neutron diffraction studies clearly evidenced the microscopic coexistence of the hedgehog SVC and SC [34, 35]. As the phase diagram of  $\text{CaK}(\text{Fe}_{1-x}\text{M}_x)_4\text{As}_4$  is revealed to be similar to that of doped 122 systems [33], it is interesting to search for a QCP in the new system.

In this Letter, we show the experimental evidence which suggests that a hidden AFM QCP exists around  $x = 0$  from systematic  $^{75}\text{As}$  NMR measurements on  $\text{CaK}(\text{Fe}_{1-x}\text{Ni}_x)_4\text{As}_4$  single crystals. In particular, this is the first indication of a QCP with the newly discovered hedgehog SVC state. Nematic order and associated fluctuations, as well as the disorder caused by substitution, are absent in the stoichiometric SC  $\text{CaKFe}_4\text{As}_4$  [36]. This makes  $\text{CaKFe}_4\text{As}_4$  ideal for investigation into the potential link between spin fluctuations and superconductivity near the QCP without any effects from the nematic fluctuations and/or disorder [37]. The details of the NMR spectrum and nuclear spin-lattice relaxation rate  $1/T_1$  data in the hedgehog SVC magnetic state for  $x = 0.049$  and also in the SC state for  $x = 0$  have been reported previously [28, 34]. In this paper, we mainly report the NMR data in the paramagnetic (PM) state and discuss the evolution of the hedgehog SVC spin correla-

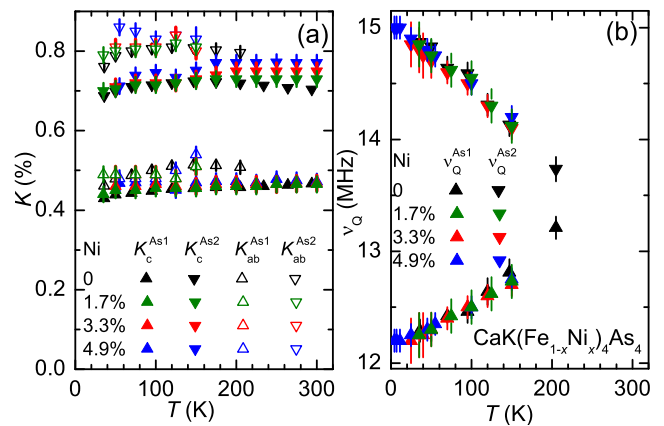


FIG. 3: (a)  $T$  dependences of the  $^{75}\text{As}$ -NMR shifts  $K_c$  and  $K_{ab}$  for the As1 and As2 sites. (b)  $T$  dependences of quadrupole frequency  $\nu_Q$  for the As1 and the As2 sites estimated from the NMR spectra.

tions with Ni substitution.

Single crystals of  $\text{CaK}(\text{Fe}_{1-x}\text{Ni}_x)_4\text{As}_4$  for the NMR measurements were grown out of a high-temperature solution rich in transition-metals and arsenic [26, 33, 38]. Ni concentration was determined by WDS [33]. NMR measurements of  $^{75}\text{As}$  ( $I = \frac{3}{2}$ ,  $\frac{\gamma_N}{2\pi} = 7.2919 \text{ MHz/T}$ ,  $Q = 0.29$  barns) nuclei were conducted using a lab-built phase-coherent spin-echo pulse spectrometer on four different compounds, pure ( $T_c = 35 \text{ K}$ ) and 1.7% substitution ( $T_c = 31 \text{ K}$ ), 3.3% substitution ( $T_c = 23 \text{ K}$ ,  $T_N = 45 \text{ K}$ ), and 4.9% substitution ( $T_c = 10 \text{ K}$ ,  $T_N = 52 \text{ K}$ ) [33]. The  $^{75}\text{As}$ -NMR spectra were obtained by sweeping the magnetic field  $H$  at fixed frequencies. The  $^{75}\text{As}$   $1/T_1$  was measured with a saturation recovery method [39].

Figures 2 (a) and (b) show the typical field-swept  $^{75}\text{As}$ -NMR spectra of  $\text{CaK}(\text{Fe}_{1-x}\text{Ni}_x)_4\text{As}_4$  in the PM state for two magnetic field directions,  $H \parallel c$  axis and  $H \parallel ab$  plane, respectively. As reported in the previous papers [28, 33, 34], the two sets of  $I = 3/2$  quadrupole split lines, corresponding to the two inequivalent As sites, are observed for the four compounds as shown in Fig. 2. The lower field central peak with a greater Knight shift  $K$  (and also larger quadrupole frequency,  $\nu_Q$ ) has been assigned to the As2 site close the Ca layers and the higher field central peak with a smaller  $K$  (and also smaller  $\nu_Q$ ) has been attributed to the As1 site close to the K layers [28]. The clear separation of the two As NMR lines indicates that the well ordered K and Ca layers are not disturbed by Ni substitution.

Figures 3 (a) and (b) show the  $T$  dependence of  $K_{ab}$  ( $H \parallel ab$  plane),  $K_c$  ( $H \parallel c$  axis) and  $\nu_Q$  for the two As sites. The As2 site  $K$ -values are uniformly higher than the As1 site  $K$ -values over the full temperature range. Due to the poor signal intensity at high  $T$ ,  $\nu_Q$  and  $K_{ab}$  can only be determined precisely up to 150–200 K.  $K_c$ , though, can be determined up to 300 K. For both the As sites, the  $K$ -

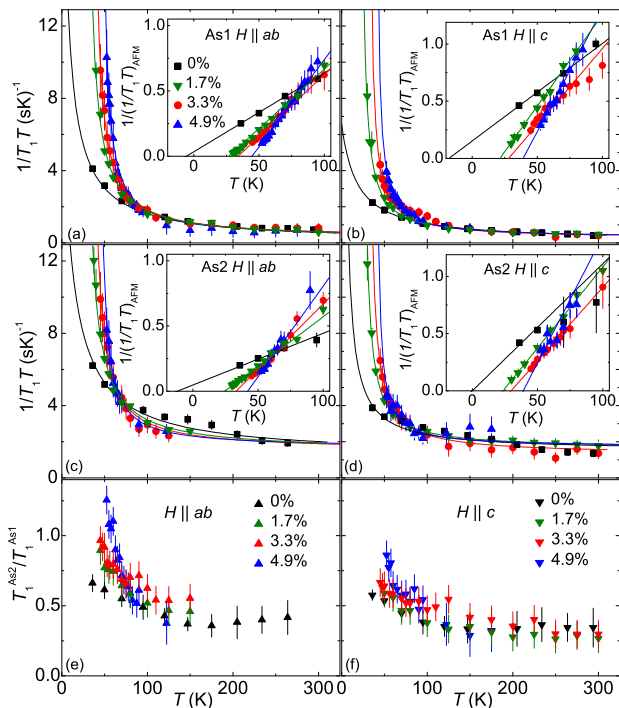


FIG. 4:  $T$  dependence of  $1/T_1T$  of As1 site for  $H \parallel ab$  plane (a) and  $H \parallel c$  axis (b), As2 site for  $H \parallel ab$  plane (c) and  $H \parallel c$  axis (d). The solid lines represent fits to  $1/T_1T = C/(T + \theta) + \text{constant}$  (see text). Inset: Inverse of the temperature dependent component of  $1/T_1T$ . The intercepts of the linear fits with the  $x$  axis correspond to  $-\theta$  (see text).  $T$  dependences of  $T_1^{\text{As2}}/T_1^{\text{As1}}$  for  $H \parallel ab$  plane (e), and  $H \parallel c$  axis (f).

values are nearly independent of  $T$ , and also nearly independent of Ni substitution, indicating that static uniform magnetic susceptibility is nearly independent of both  $T$  and  $x$ , although the ground states vary from magnetic to nonmagnetic. These data also suggest that Ni substitution up to 4.9% does not produce significant change in the density of states at the Fermi energy  $N(E_F)$ .

The  $T$  dependences of  $\nu_Q$  of As1 and As2 in  $\text{CaK}(\text{Fe}_{1-x}\text{Ni}_x)_4\text{As}_4$  are shown in Fig. 3(b). Similar to the  $K$  data,  $\nu_Q$  is almost independent of Ni substitution. All the As2  $\nu_Q$ -values are larger than the As1  $\nu_Q$ -values. For all the samples, with increasing  $T$ ,  $\nu_Q$  of As1 increases, while  $\nu_Q$  of As2 shows an opposite trend. The different  $T$  dependences of the values of  $\nu_Q$  for the two As sites have been ascribed to hedgehog SVC magnetic fluctuations [28].

Figures 4 (a) - (d) show the  $T$  dependence of  $1/T_1T$  for the two As sites under the different magnetic field directions. As can be seen, all  $1/T_1T$  plots increase with decreasing  $T$ .  $1/T_1T$  can be expressed in terms of the imaginary part of the dynamic susceptibility  $\chi''(\vec{q}, \omega_0)$  at the Larmor frequency  $\omega_0$  per mole of electronic spins as [40],  $\frac{1}{T_1T} = \frac{2\gamma_N^2 k_B}{N_A} \sum_{\vec{q}} |A(\vec{q})|^2 \frac{\chi''(\vec{q}, \omega_0)}{\omega_0}$ , where the sum is over the wave vectors  $\vec{q}$  within the first Brillouin zone,  $A(\vec{q})$

is the form factor of the hyperfine interactions. On the other hand,  $K$  reflects the  $q = 0$  component of magnetic susceptibility  $\chi'(\vec{q}, \omega_0)$ . Therefore, the enhancement of  $1/T_1T$  at low  $T$  where  $K$  is almost constant indicates a growth of AFM spin correlations with  $q \neq 0$ .

According to the previous analysis of  $1/T_1T$  for  $x = 0$  and 0.049 [28, 34], the AFM spin correlations can be characterized to be hedgehog SVC correlations experimentally by the  $T$  dependence of the ratio of  $1/T_1$  for As1 and  $1/T_1$  for As2 [Figs. 4(e) and (f)]. In the hedgehog SVC ordered state, the internal magnetic induction  $B_{\text{int}}$  at As1 is finite along the  $c$  axis while the  $B_{\text{int}}$  at As2 is zero due to a cancellation originating from the characteristic spin structure [33, 34]. Therefore, one expects that  $1/T_1$  for As1 is enhanced compared to that of As2 if the AFM spin fluctuations originate from the hedgehog SVC-type spin correlations. For stripe-type AFM fluctuations, the  $T$  dependence of  $1/T_1$  for As1 should scale to that of  $1/T_1$  for As2 since there is no cancellation of the internal induction at either As site [33]. As can be seen in Figs. 4(e) and (f), the ratios of  $T_1^{\text{As2}}/T_1^{\text{As1}}$  show a nearly  $T$  independent value of  $\sim 0.3$ – $0.4$  above 150 K, which could be determined by the different hyperfine coupling constants for the As1 and As2 sites. Below 150 K, clear enhancements of  $T_1^{\text{As2}}/T_1^{\text{As1}}$  are observed. These results indicate that the As1 sites experience stronger AFM spin fluctuations than the As2 sites, consistent with the growth of the hedgehog SVC spin fluctuations.

In order to get more insight into the hedgehog SVC spin fluctuations, we analyze the  $1/T_1T$  data using a phenomenological model where  $1/T_1T$  is decomposed into two components:  $1/T_1T = (1/T_1T)_{\text{AFM}} + (1/T_1T)_0$  [12–15, 41]. Here,  $(1/T_1T)_{\text{AFM}}$  is due to the AFM spin fluctuations which can be described by a Curie-Weiss (CW) formula  $(1/T_1T)_{\text{AFM}} = C/(T + \theta)$  expected for an AFM spin fluctuation for a two-dimensional (2D) system from the self-consistent renormalization theory [40]. The Curie constant  $C$  measures the spectral weight of AFM fluctuations and the Weiss temperature  $\theta$  corresponds to the distance from the AFM instability point. For the other term originating from a contribution other than the AFM correlations, we assumed  $(1/T_1T)_0 = \text{constant}$  which is expected for Korringa relation of  $T_1TK^2 = \text{constant}$  since  $K$  is nearly constant. The solid lines in Figs. 4 (a)-(d) are fits for all  $1/T_1T$  data. The CW behavior of  $(1/T_1T)_{\text{AFM}}$  can be also seen clearly in the insets for each figure where the inverse of  $(1/T_1T)_{\text{AFM}}$  follows  $T$  linear dependence.

Figure 5 shows the  $x$  dependence of  $\theta$  and  $C$  estimated from the fits, together with the phase diagram of  $\text{CaK}(\text{Fe}_{1-x}\text{Ni}_x)_4\text{As}_4$  [33]. As shown in the bottom panel, as  $x$  decreases,  $C$  increases and  $\theta$  approaches zero. The increase of  $C$  suggests enhancement of the AFM fluctuations. A similar trend of  $T_c$  is observed, suggesting a correlation between  $C$  and  $T_c$ . On the other hand, as shown above,  $N(E_F)$  in  $\text{CaK}(\text{Fe}_{1-x}\text{Ni}_x)_4\text{As}_4$  changes little upon  $x$ , while  $T_c$  decreases as  $x$  increases. This is

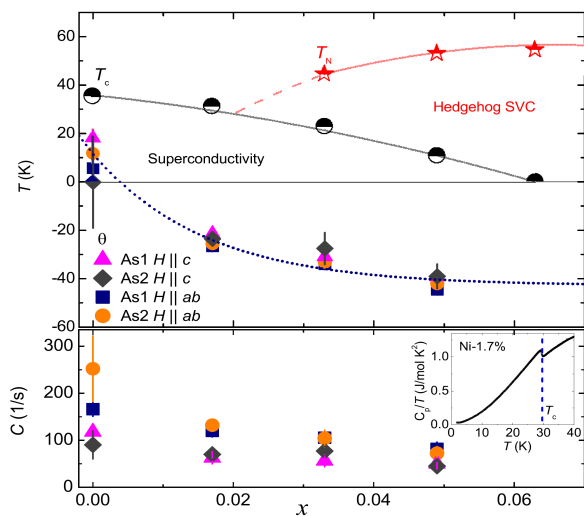


FIG. 5: Phase diagram of Ni doped  $\text{CaKFe}_4\text{As}_4$  (Top).  $T_N$  and  $T_c$  are from Ref. 33. Weiss temperature  $\theta$  and Curie constant  $C$  (Bottom) are obtained from the fits in Fig. 4. The lines are the guides to the eyes. The inset of the bottom panel shows the specific heat  $C_p/T$  of Ni-1.7% sample.

in contrast to the conventional BCS superconductors, in which  $N(E_F)$  generally correlates with  $T_c$ . These results strongly, therefore, indicate that the hedgehog SVC spin fluctuations play an important role in the appearance of SC in  $\text{CaKFe}_4\text{As}_4$ .  $\theta = 0$  K implies that the compound would show a hedgehog SVC magnetic order at 0 K *if it remained in the normal state*. This is an indication of an AFM QCP around  $x = 0$  which is hidden or, as shown below, shifted by the appearance of SC below  $T_c$ .

In general, one expects that a magnetic QCP exists in proximity to an AFM phase boundary. For  $\text{CaK}(\text{Fe}_{1-x}\text{Ni}_x)_4\text{As}_4$ , therefore, an AFM state may be expected in the Ni-1.7% sample whose  $T_N$  is expected to be lower than  $T_c$  from a simple extrapolation of the values of  $T_N$  of the higher Ni concentration compounds. As shown in Figs. 3 (a)-(d), the strong divergent behavior in  $1/T_1T$  with the negative  $\theta$  value observed in the  $T > T_c$  data for Ni-1.7% sample is very similar to those observed at  $T_N$  for Ni-3.3% and 4.9% samples, suggesting an AFM order in the Ni-1.7% doped sample. The NMR spectrum measurements below  $T_c$  in Ni-1.7% sample were difficult to determine the ground state due to the poor NMR signal intensity originating from Meissner effect. However, as shown in the inset of the bottom panel of Fig. 5, specific-heat ( $C_p$ ) measurements do not show any evidence of magnetic order below  $T_c$  in the Ni-1.7% doped sample where the clear jump in  $C_p$  at  $T_c$  can be detected [44]. These results indicate that no static magnetic order is established in the Ni-1.7% sample below  $T_c$  and in a similar manner there is no magnetic order expected for  $x \leq 0.017$ . Similar sudden disappearance of the AFM state in SC state has been observed

in 122 families where the  $T_N$  line bent backwards into the AFM region [2]. The absence of the magnetic order may originate from the strong competition with SC order in this region. The disappearance of magnetic order and/or the backbending behavior of  $T_N$  have been discussed theoretically based on Ginzburg-Landau theory [45]. Although the actual AFM phase boundary in SC state at low Ni-substitution levels does not change our conclusion of the hidden QCP around  $x = 0$ , which is revealed from the  $1/T_1T$  data in the normal state, it is interesting and important to reveal the details of the phase diagram of  $\text{CaK}(\text{Fe}_{1-x}\text{Ni}_x)_4\text{As}_4$ . It would also be of great interest to investigate how the phase boundary changes if the SC is suppressed, for example, by strong magnetic field.

It is generally believed that, in proximity to an AFM QCP, the scattering process of quasiparticles is strongly affected by the quantum fluctuations, leading to non-Fermi-liquid behavior. As a result, electrical resistivity ( $\rho$ ) increases linearly with temperature, which has been actually observed in high- $T_c$  cuprates and some iron-based SCs around a QCP [7, 9, 11, 12, 15]. In the case of  $\text{CaKFe}_4\text{As}_4$  [26], on the other hand,  $\rho$  is observed to be proportional to  $T^{1.5}$  whose exponent is slightly higher than unity, but is clearly smaller than two expected for conventional Fermi liquid. Recently, the  $T$ -linear scattering rate of the coherent response [42] as a result of quantum fluctuations has been observed by an optical conductivity study of  $\text{CaKFe}_4\text{As}_4$  [43], although the  $T$ -linear  $\rho$  is not observed. These results also support an existence of a magnetic QCP associated with the  $T > T_c$  normal state, around  $\text{CaKFe}_4\text{As}_4$ .

The possibility of the avoided magnetic QCP in doped 122 compounds has been suggested by the observation of a distribution of  $T_1$  and also of a secondary incommensurate magnetic phase near the optimal  $T_c$  [16–21]. In the case of  $\text{CaKFe}_4\text{As}_4$ , it is important to point out that we do not observe any distribution of  $T_1$  in the normal state, indicative of no significant inhomogeneity. In addition, bulk measurements,  $\mu\text{SR}$  and neutron scattering as well as NMR also rule out any magnetic phase in  $\text{CaKFe}_4\text{As}_4$  [26–29]. Therefore the stoichiometric  $\text{CaKFe}_4\text{As}_4$  provides a unique opportunity to explore quantum criticality without the inherent substitutional disorder in analogous doped 122 systems.  $\text{AFe}_2\text{As}_2$  ( $A = \text{K}, \text{Rb}, \text{Cs}$ ) [46, 47] and  $\text{LiFeAs}$  [48] are stoichiometric superconductors as well, and those systems are pointed out to be presumably located close to a magnetic instability. However, the maximum  $T_c$  in  $\text{Ba}_{1-x}\text{K}_x\text{Fe}_2\text{As}_2$  appears at  $x \sim 0.4$ , not at the stoichiometric composition.  $\text{LiFeAs}$  shows a Fermi-liquid behavior, and no magnetic transitions has been detected in the temperature-doping ( $T$ - $x$ ) phase diagram of  $\text{LiFe}_{1-x}\text{Co}_x\text{As}$  [49]. These are quite different from  $\text{CaK}(\text{Fe}_{1-x}\text{Ni}_x)_4\text{As}_4$ .

In summary, our  $^{75}\text{As}$  NMR measurements of  $\text{CaK}(\text{Fe}_{1-x}\text{Ni}_x)_4\text{As}_4$  provide evidence for a QCP asso-



ciated with hedgehog SVC fluctuations near  $x = 0$ . In contrast to other reported iron-based SCs with QCP, stoichiometric  $\text{CaKFe}_4\text{As}_4$  is free of the substitutional disorder from chemical doping and also nematic transition. The magnetic QCP without accompanying nematicity in  $\text{CaK}(\text{Fe}_{1-x}\text{Ni}_x)_4\text{As}_4$  highlights the close connection of spin fluctuations and SC in iron-based SCs. These advantages makes  $\text{CaKFe}_4\text{As}_4$  an ideal platform to investigate the relationship between magnetic QCP and SC in iron-based SCs.

We thank P. Wiecki for helpful discussions. The research was supported by the U.S. Department of Energy (DOE), Office of Basic Energy Sciences, Division of Materials Sciences and Engineering. Ames Laboratory is operated for the U.S. DOE by Iowa State University under Contract No. DE-AC02-07CH11358. W.R.M. was supported by the Gordon and Betty Moore Foundation's EPIQS Initiative through Grant No. GBMF4411.

- 
- [1] P. C. Canfield and S. L. Bud'ko, *Annu. Rev. Condens. Matter Phys.* **1**, 27 (2010).
- [2] D. C. Johnston, *Adv. Phys.* **59**, 803 (2010).
- [3] P. J. Hirschfeld, M. M. Korshunov, and I. I. Mazin, *Rep. Prog. Phys.* **74**, 124508 (2011).
- [4] G. R. Stewart, *Rev. Mod. Phys.* **83**, 1589 (2011).
- [5] M. R. Norman, D. Pines, C. Kallin, *Adv. Phys.* **54**, 715 (2005).
- [6] C. Pfleiderer, *Rev. Mod. Phys.* **81**, 1551 (2009).
- [7] D. M. Broun, *Nat. Phys.* **4**, 170 (2008).
- [8] J. Dai, Q. Si, J.-X. Zhu, E. Abrahams, *Proc. Natl. Acad. Sci. U.S.A.* **106**, 4118 (2009).
- [9] T. Shibauchi, A. Carrington, and Y. Matsuda, 2014, *Annu. Rev. Condens. Matter Phys.* **5**, 113 (2014).
- [10] S. Sachdev, *Quantum Phase Transitions* (Cambridge University Press, Cambridge, England, 1999).
- [11] S. Sachdev, B. Keimer, *Phys. Today* **64**, 29 (2011).
- [12] Y. Nakai, T. Iye, S. Kitagawa, K. Ishida, H. Ikeda, S. Kasahara, H. Shishido, T. Shibauchi, Y. Matsuda, and T. Terashima, *Phys. Rev. Lett.* **105**, 107003 (2010).
- [13] F. L. Ning, K. Ahilan, T. Imai, A. S. Sefat, R. Jin, M. A. McQuire, B. C. Sales, and D. Mandrus, *J. Phys. Soc. Jpn.* **78**, 013711 (2009).
- [14] F. L. Ning, K. Ahilan, T. Imai, A. S. Sefat, M. A. McGuire, B. C. Sales, D. Mandrus, P. Cheng, B. Shen, and H.-H. Wen, *Phys. Rev. Lett.* **104**, 037001 (2010).
- [15] R. Zhou, Z. Li, J. Yang, D. L. Sun, C. T. Lin, and G.-q. Zheng, *Nat. Commun.* **4**, 2265 (2013).
- [16] A. P. Dioguardi, J. Crocker, A. C. Shockley, C. H. Lin, K. R. Shirer, D. M. Nisson, M. M. Lawson, N. apRoberts-Warren, P. C. Canfield, S. L. Bud'ko, S. Ran, and N. J. Curro, *Phys. Rev. Lett.* **111**, 207201 (2013).
- [17] X. Lu, D. W. Tam, C. Zhang, H. Luo, M. Wang, R. Zhang, L. W. Harriger, T. Keller, B. Keimer, L.-P. Regnault, T. A. Maier, and P. Dai, *Phys. Rev. B* **90**, 024509 (2014).
- [18] C. Bernhard, C. N. Wang, L. Nuccio, L. Schulz, O. Zaharko, J. Larsen, C. Aristizabal, M. Willis, A. J. Drew, G. D. Varma, T. Wolf, and Ch. Niedermayer, *Phys. Rev. B* **86**, 184509 (2012).
- [19] H. Luo, R. Zhang, M. Laver, Z. Yamani, M. Wang, X. Lu, M. Wang, Y. Chen, S. Li, S. Chang, J. W. Lynn, and P. Dai, *Phys. Rev. Lett.* **108**, 247002 (2012).
- [20] X. Lu, H. Gretarsson, R. Zhang, X. Liu, H. Luo, W. Tian, M. Laver, Z. Yamani, Y.-J. Kim, A. H. Nevidomskyy, Q. Si, and P. Dai, *Phys. Rev. Lett.* **110**, 257001 (2013).
- [21] D. Hu, X. Lu, W. Zhang, H. Luo, S. Li, P. Wang, G. Chen, F. Han, S. R. Banjara, A. Sapkota, A. Kreyssig, A. I. Goldman, Z. Yamani, C. Niedermayer, M. Skoulatos, R. Georgii, T. Keller, P. Wang, W. Yu, and P. Dai, *Phys. Rev. Lett.* **114**, 157002 (2015).
- [22] S. Lederer, Y. Schattner, E. Berg, and S. A. Kivelson, *Phys. Rev. Lett.* **114**, 097001 (2015).
- [23] Y. Schattner, S. Lederer, S. A. Kivelson, and E. Berg, *Phys. Rev. X* **6**, 031028 (2016).
- [24] Z. Liu, Y. Gu, W. Zhang, D. Gong, W. Zhang, T. Xie, X. Lu, X. Ma, X. Zhang, R. Zhang, J. Zhu, C. Ren, L. Shan, X. Qiu, P. Dai, Y.-f. Yang, H. Luo, and S. Li, *Phys. Rev. Lett.* **117**, 157002 (2016).
- [25] A. Iyo, K. Kawashima, T. Kinjo, T. Nishio, S. Ishida, H. Fujihisa, Y. Gotoh, K. Kihou, H. Eisaki, and Y. Yoshida, *J. Am. Chem. Soc.* **138**, 3410 (2016).
- [26] W. R. Meier, T. Kong, U. S. Kaluarachchi, V. Taufour, N. H. Jo, G. Drachuck, A. E. Böhmer, S. M. Saunders, A. Sapkota, A. Kreyssig, M. A. Tanatar, R. Prozorov, A. I. Goldman, F. F. Balakirev, A. Gurevich, S. L. Bud'ko, and P. C. Canfield, *Phys. Rev. B* **94**, 064501 (2016).
- [27] T. Xie, Y. Wei, D. Gong, T. Fennell, U. Stuhr, R. Kajimoto, K. Ikeuchi, S. Li, J. Hu, and H. Luo, *Phys. Rev. Lett.* **120**, 267003 (2018).
- [28] J. Cui, Q.-P. Ding, W. R. Meier, A. E. Böhmer, T. Kong, V. Borisov, Y. Lee, S. L. Bud'ko, R. Valentí, P. C. Canfield, and Y. Furukawa, *Phys. Rev. B* **96**, 104512 (2017).
- [29] P. K. Biswas, A. Iyo, Y. Yoshida, H. Eisaki, K. Kawashima and A. D. Hillier, *Phys. Rev. B* **95**, 140505 (2017).
- [30] K. Cho, A. Fente, S. Teknowijoyo, M. A. Tanatar, K. R. Joshi, N. M. Nusran, T. Kong, W. R. Meier, U. Kaluarachchi, I. Guillamón, H. Suderow, S. L. Bud'ko, P. C. Canfield and R. Prozorov, *Phys. Rev. B* **95**, 100502 (2017).
- [31] D. Mou, T. Kong, W. R. Meier, F. Lochner, L.-L. Wang, Q. Lin, Y. Wu, S. L. Bud'ko, I. Eremin, D. D. Johnson, P. C. Canfield, and A. Kaminski, *Phys. Rev. Lett.* **117**, 277001 (2016).
- [32] K. Iida, M. Ishikado, Y. Nagai, H. Yoshida, A. D. Christianson, N. Murai, K. Kawashima, Y. Yoshida, H. Eisaki, and A. Iyo, *J. Phys. Soc. Jpn.* **86**, 093703 (2017).
- [33] W. R. Meier, Q.-P. Ding, A. Kreyssig, S. L. Bud'ko, A. Sapkota, K. Kothapalli, V. Borisov, R. Valentí, C. D. Batista, P. P. Orth, R. M. Fernandes, A. I. Goldman, Y. Furukawa, A. E. Böhmer, and P. C. Canfield, *npj Quant. Mater.* **3**, 5 (2018).
- [34] Q.-P. Ding, W. R. Meier, A. E. Böhmer, S. L. Bud'ko, P. C. Canfield, and Y. Furukawa, *Phys. Rev. B* **96**, 220510(R) (2017).
- [35] A. Kreyssig, J. M. Wilde, A. E. Böhmer, W. Tian, W. R. Meier, B. Li, B. G. Ueland, M. Xu, S. L. Bud'ko, P. C. Canfield, R. J. McQueeney, and A. I. Goldman, *Phys. Rev. B* **97**, 224521 (2018).
- [36] W.-L. Zhang, W. R. Meier, T. Kong, P. C. Canfield, and G. Blumberg, arXiv:1804.06963.
- [37] Y. Gu, Z. Liu, T. Xie, W. Zhang, D. Gong, D. Hu, X.

- Ma, C. Li, L. Zhao, L. Lin, Z. Xu, G. Tan, G. Chen, Z. Y. Meng, Y.-f. Yang, H. Luo, and S. Li, *Phys. Rev. Lett.* **119**, 157001 (2017).
- [38] W. R. Meier, T. Kong, S. L. Bud'ko, and P. C. Canfield, *Phys. Rev. Mater.* **1**, 013401 (2017).
- [39] See Supplemental Material for details for the determination of  $T_1$  and the position dependence of  $T_1$ .
- [40] T. Moriya, *J. Phys. Soc. Jpn.* **18**, 516 (1963).
- [41] J. Cui, B. Roy, M. A. Tanatar, S. Ran, S. L. Bud'ko, R. Prozorov, P. C. Canfield and Y. Furukawa, *Phys. Rev. B* **92**, 184504 (2015).
- [42] Y. M. Dai, B. Xu, B. Shen, H. Xiao, H. H. Wen, X. G. Qiu, C. C. Homes, and R. P. S. M. Lobo, *Phys. Rev. Lett.* **111**, 117001 (2013).
- [43] R. Yang, Y. Dai, B. Xu, W. Zhang, Z. Qiu, Q. Sui, C. C. Homes, and X. Qiu, *Phys. Rev. B* **95**, 064506 (2017).
- [44] The heat capacity data of the Ni-1.7% sample was measured using a hybrid adiabatic relaxation technique of the heat capacity option in a Quantum Design, Physical Properties Measurement System.
- [45] R. M. Fernandes, and J. Schmalian, *Phys. Rev. B* **82**, 014521 (2010).
- [46] Z. T. Zhang, D. Dmytriieva, S. Molatta, J. Wosnitza, S. Khim, S. Gass, A. U. B. Wolter, S. Wurmehl, H.-J. Grafe, and H. Kühne, *Phys. Rev. B* **97**, 115110 (2018).
- [47] Y. P. Wu, D. Zhao, A. F. Wang, N. Z. Wang, Z. J. Xiang, X. G. Luo, T. Wu, and X. H. Chen, *Phys. Rev. Lett.* **116**, 147001 (2016).
- [48] S.-H. Baek, L. Harnagea, S. Wurmehl, B. Büchner, and H.-J. Grafe, *J. Phys.: Condens. Matter* **25**, 162204 (2013).
- [49] Y. M. Dai, H. Miao, L. Y. Xing, X. C. Wang, P. S. Wang, H. Xiao, T. Qian, P. Richard, X. G. Qiu, W. Yu, C. Q. Jin, Z. Wang, P. D. Johnson, C. C. Homes, and H. Ding, *Phys. Rev. X* **5**, 031035 (2015).